

Learning A Physical-aware Diffusion Model Based on Transformer for Underwater Image Enhancement

Chen Zhao*
Nanjing Normal University
Nanjing, China
2518628273@qq.com

Chenyu Dong*
Nanjing Normal University
Nanjing, China
546845583@qq.com

Weiling Cai
Nanjing Normal University
Nanjing, China
24577075@qq.com

ABSTRACT

Underwater visuals undergo various complex degradations, inevitably influencing the efficiency of underwater vision tasks. Recently, diffusion models were employed to underwater image enhancement (UIE) tasks, and gained SOTA performance. However, these methods fail to consider the physical properties and underwater imaging mechanisms in the diffusion process, limiting information completion capacity of diffusion models. In this paper, we introduce a novel UIE framework, named PA-Diff, designed to exploiting the knowledge of physics to guide the diffusion process. PA-Diff consists of Physics Prior Generation (PPG) Branch, Implicit Neural Reconstruction (INR) Branch, and Physics-aware Diffusion Transformer (PDT) Branch. Our designed PPG branch aims to produce the prior knowledge of physics. With utilizing the physics prior knowledge to guide the diffusion process, PDT branch can obtain underwater-aware ability and model the complex distribution in real-world underwater scenes. INR Branch can learn robust feature representations from diverse underwater image via implicit neural representation, which reduces the difficulty of restoration for PDT branch. Extensive experiments prove that our method achieves best performance on UIE tasks. The code is available at <https://github.com/chenyudong/PA-Diff>.

CCS CONCEPTS

• **Computing methodologies** → **Artificial intelligence; Computer vision;**

KEYWORDS

Underwater image enhancement, Physics model, Diffusion model, Transformer

ACM Reference Format:

Chen Zhao[1], Chenyu Dong[1], and Weiling Cai. 2018. Learning A Physical-aware Diffusion Model Based on Transformer for Underwater Image Enhancement. In *Proceedings of Make sure to enter the correct conference title from your rights confirmation email (MM'24)Proceedings of the 32nd ACM International Conference on Multimedia (MM'24)*, October 28-November 1, 2024, Melbourne, Australia. ACM, New York, NY, USA, 10 pages. <https://doi.org/XXXXXXX.XXXXXXX>

Permission to make digital or hard copies of all or part of this work for personal or classroom use is granted without fee provided that copies are not made or distributed for profit or commercial advantage and that copies bear this notice and the full citation on the first page. Copyrights for components of this work owned by others than the author(s) must be honored. Abstracting with credit is permitted. To copy otherwise, or republish, to post on servers or to redistribute to lists, requires prior specific permission and/or a fee. Request permissions from permissions@acm.org.
MM'24, October 28 - November 1, 2024, Melbourne, Australia.

© 2018 Copyright held by the owner/author(s). Publication rights licensed to ACM.
ACM ISBN 978-1-4503-XXXX-X/18/06
<https://doi.org/XXXXXXX.XXXXXXX>

1 INTRODUCTION

The restoration of images beneath the water's surface is a pragmatic yet intricate technology within the realm of underwater vision, extensively applied in endeavors such as underwater robotics[29] and tracking underwater objects[11]. Owing to the phenomena of light refraction, absorption, and scattering in underwater surroundings, images captured underwater are often subject to substantial distortion, characterized by diminished contrast and inherent blurriness [3]. Consequently, the primary objective of underwater image enhancement (UIE) lies in the attainment of superior-quality images, achieved through the elimination of scattering effects and rectification of color distortions prevalent in degraded images.

To address this problem, conventional UIE approaches, which hinge on the intrinsic characteristics of underwater images, have been presented [20, 35, 36]. These techniques delve into the physical aspects contributing to degradation, such as color cast or scattering, seeking to rectify and enhance the underwater images. Nevertheless, these models grounded in physics exhibit restricted representational capacities, rendering them insufficient for comprehensively addressing the intricate physical and optical elements inherent in underwater scenes. Consequently, their efficacy diminishes, yielding suboptimal enhancement outcomes, particularly in the face of highly intricate and diverse underwater scenarios.

In recent times, many learning-based methodologies [14, 24, 34, 44] have been introduced to yield superior results. Leveraging the potent feature representation and nonlinear mapping capabilities of neural networks, these methods excel. Deep learning-based methods can be roughly categorized into two classes: physics-free end-to-end methods [19, 34] and physics-aware methods [15, 23, 31]. Regarding the physics-free end-to-end methods, most of them usually use ground-truth images as labels to enforce L1/L2 distance-based consistency and also introduce various regularizations as additional constraints to deal with the ill-posed property. Although these methods achieve decent performance, they mainly consider the model in the raw image space, which does not fully explore the useful physics-aware feature information for UIE. Regarding the physics-aware deep methods, most of them utilize the atmospheric scattering model. Existing UIE approaches [15, 23] develop deep neural networks to estimate the transmission and the background scattered light, and then follow the traditional UIE methods to restore underwater images. However, these approaches do not correct the errors of the atmospheric light estimated by neural networks, which seriously affects the quality of the images [53]. Therefore, there is a crucial problem to adequately exploit the physical information and effectively incorporate them into a unified UIE deep framework.

¹These authors contributed equally to this work.

Recently, there has been a surge of interest in image synthesis [26, 27, 38, 40, 60] and restoration tasks [10, 47, 54, 61], with a notable focus on diffusion-based techniques like DDPM [18] and DDIM [41]. This heightened attention can be attributed to the remarkable generative capabilities of diffusion models. These methods can gradually recover images from noisy images generated in the forward diffusion process and achieve high-quality mapping from randomly sampled Gaussian noise to target images in the reverse diffusion process [18], which poses a new perspective for underwater image enhancement task. Tang et al. [44] present an image enhancement approach with diffusion model in underwater scenes, and WF-Diff [57] proposed a underwater image enhancement framework based on frequency domain information and diffusion models. UIEDP propose a UIE framework with Diffusion Prior, treating UIE as a posterior distribution sampling process of clear images conditioned on degraded underwater inputs [13]. However, these methods fail to consider the physical properties and underwater imaging mechanisms in the diffusion process, limiting their information completion capacity for the diffusion model. Moreover, the diffusion models lack awareness regarding the difficulty of enhancing different image regions, a critical consideration for modeling the complex distribution in real-world underwater scenes.

In this paper, we develop a novel physics-aware diffusion model, fully exploiting physical information to guide the diffusion process, called PA-Diff. It mainly consists of three branches: Physics Prior Generation (PPG) Branch, Implicit Neural Reconstruction (INR) Branch, and Physics-aware Diffusion Transformer (PDT) Branch. The PPG branch aims to generate the transmission map and the global background light as physics prior information by utilizing the modified koschmieder light scanning model [1]. The transmission map is exploited as the confidence guidance for the PDT branch which enables our PA-Diff with underwater-aware ability. The global background light can be regarded as a prior condition on both the type and degree of degradation for the PDT Branch. Inspired by the latest works [6, 50] based on INR that can encode an image as a continuous function and learn a more robust degradation representation, we further incorporate the INR into our proposed framework to learn robust feature representations from diverse underwater image. The PDT branch employs the strong generation ability of diffusion models to restore underwater images, with the guidance of physical information. Specifically, we design a physics-aware diffusion transformer block which contain a physics-aware self-attention (PA-SA), physics perception unit (PPU) and gated multi-scale feed-forward network (GM-FFN) to exploit physics prior information and capture the long-range diffusion dependencies. Our PA-Diff achieves unprecedented perceptual performance in UIE task. Extensive experiments demonstrate that our developed PA-Diff performs the superiority against previous UIE approaches, and ablation study can demonstrate the effectiveness of all contributions.

In summary, the main contributions of our PA-Diff are as follows:

- We propose a novel UIE framework based on physics-aware diffusion model, named PA-Diff, which consists of Physics Prior Generation (PPG) Branch, Implicit Neural Reconstruction (INR) Branch, and Physics-aware Diffusion Transformer (PDT) Branch. To the best of our knowledge, it is the first the
- Diffusion model with the guidance of physical knowledge in underwater image enhancement tasks.
- We incorporate Implicit Neural Reconstruction into our proposed PA-Diff to learn robust feature representations from diverse underwater image, which reduces the difficulty of restoration for diffusion models.
- We design a physics-aware diffusion transformer block, which not only enables PA-Diff with underwater-aware ability to guide the diffusion process, but also captures the long-range diffusion dependencies. Moreover, we also propose a physics perception unit (PPU), which can explore the beneficial feature-level physics information for underwater image enhancement.
- Extensive experiments compared with SOTAs considerably demonstrate that our PA-Diff performs the superiority against previous UIE approaches, and extensive ablation experiments can demonstrate the effectiveness of all contributions.

2 RELATED WORKS

2.1 Underwater Image Enhancement

Currently, existing UID methods can be briefly categorized into the physical and deep model-based approaches [24, 34–36, 44]. Most UID methods based on the physical model utilize prior knowledge to establish models, such as water dark channel priors [36], attenuation curve priors [46], fuzzy priors [9]. In addition, Akkaynak and Treibitz [2] proposed a method based on the revised physical imaging model. However, the depth map of the underwater scene is difficult to obtain. This leads to unstable performance of the this method, which usually suffers from severe color cast and artifacts. Therefore, the manually established priors restrain the model's robustness and scalability under the complicated and varied circumstances. In recent years, underwater physical imaging models are gradually utilized in combination with data-driven methods [23]. Recently, deep learning-based methods [16, 24, 34, 44] achieve acceptable performance, and some complex frameworks are proposed and achieve the-state-of-the-art performance [20, 36, 58]. The previous methods neglect the underwater imaging mechanism and rely only on the representation ability of deep networks. Ucolor [23] combined the underwater physical imaging model in the raw space and designed a medium transmission guided model. ATDC-net [30] attempted to use transmission maps to guide deep neural networks. Therefore, how to fully exploit the knowledge of physics in deep neural networks is a very crucial problem.

2.2 Diffusion Model

Diffusion Probabilistic Models (DPMs) [18, 41] have been widely adopted for conditional image generation [10, 26, 47, 60, 61]. Saharia et al. [39] proposes Palette, which has demonstrated the excellent performance of diffusion models in the field of conditional image generation, including colorization, in-painting and JPEG restoration. Currently, diffusion models was employed to a variety of low-level visual tasks, and gained SOTA performance such as image restoration [32], document enhancement [52], and low light image enhancement [51, 61]. Recently, Tang et al. [44] presented an image enhancement approach with diffusion model in underwater scenes. WF-Diff [57] proposed a underwater image enhancement framework based on frequency domain information and diffusion

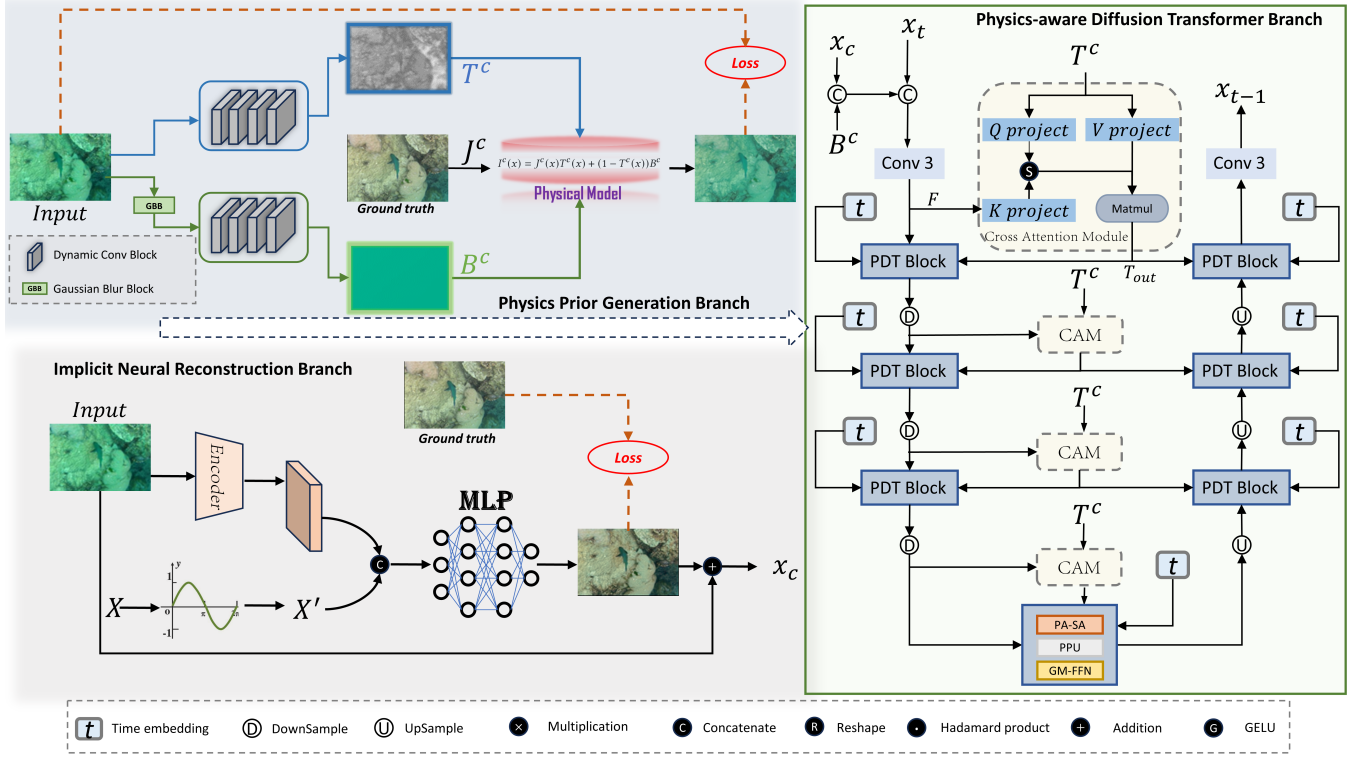


Figure 1: Overall framework of our proposed PA-Diff. PA-Diff mainly consists of three cooperative branches: **Physics Prior Generation (PPG) Branch**, **Implicit Neural Reconstruction (INR) Branch**, and **Physics-aware Diffusion Transformer (PDT) Branch**. Our designed PPG branch aims to produce the prior knowledge of physics. With utilizing the physics prior knowledge to guide the diffusion process, PDT branch can obtain underwater-aware ability and model the complex distribution in real-world underwater scenes. INR Branch can learn robust feature representations from diverse underwater image, which reduces the difficulty of restoration for diffusion models.

models. UIEDP propose a UIE framework with Diffusion Prior, treating UIE as a posterior distribution sampling process of clear images conditioned on degraded underwater inputs[13]. However, these methods fail to consider the physical properties and underwater imaging mechanisms in the diffusion process, limiting information completion capacity of diffusion models.

2.3 Implicit Neural Representation

Implicit Neural Representations (INRs) have emerged as an innovative technique garnering substantial attention for their ability to utilize coordinate-based Multi-Layer Perceptrons (MLPs) to model continuous-domain signals. Recently, some works have delved into the potential of INRs within the realm of two-dimensional image processing, including applications like image compression [42], and super-resolution[5]. Chen et al. [8] first capitalized on INRs to achieve continuous image super-resolution. Subsequently, Lee et al. [21] proposed a dominant-frequency estimator that effectively predicts local texture information in natural images. Sun et al. [43] leveraged INRs to forecast continuous attributes based on the captured tomographic features. More recently, Quan et al. [37] introduced an INR-based inverse kernel prediction network to address the problem of single image defocus deblurring. Concurrently, Yang et al. [50] exploited the controllable fitting capabilities of INRs to tackle the challenge of low-light image enhancement. Chen et al.

[6] utilized INRs to learn common rain degradation representations from diverse rainy scenes. These efforts [6, 43, 50] convincingly demonstrate the robust representation capabilities of INRs when applied to degraded images. Thus, inspired by the previous works, we explore the application of INRs to obtain robust feature representations for underwater image enhancement, aiming to reduce the difficulty of restoration for diffusion models.

3 METHODOLOGY

3.1 Overall Framework

The overall framework of PA-Diff is shown in Fig. 1. PA-Diff is designed to leverage the physical properties of underwater imaging mechanisms to guide the diffusion process, which mainly consists of Physics Prior Generation (PPG) Branch, Implicit Neural Reconstruction (INR) Branch, and Physics-aware Diffusion Transformer (PDT) Branch. The PPG branch aims to generate the transmission map and the global background light as physics prior information by utilizing the modified koschmieder light scanning model. The transmission map is exploited as the confidence guidance for the PDT branch which enables our PA-Diff with underwater-aware ability. The global background light can be regarded as a prior condition on both the type and degree of degradation for the PDT Branch. Inspired by [6, 50] based on implicit neural representations that can encode an image as a continuous function and learn a

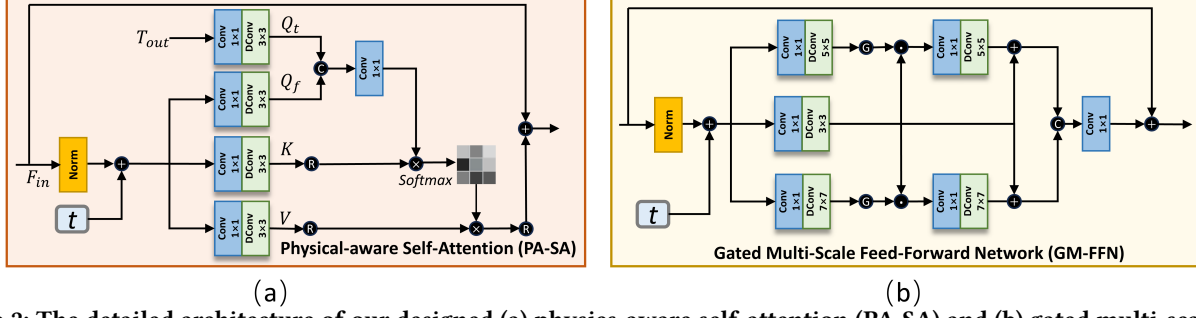


Figure 2: The detailed architecture of our designed (a) physics-aware self-attention (PA-SA) and (b) gated multi-scale feed-forward network (GM-FFN).

more robust feature representation, we further introduce implicit neural representations to learn robust degradation representations from diverse underwater image, aiming to reduce the difficulty of restoration for diffusion models. The PDT branch employs the strong generation ability of diffusion models to restore underwater images, with the guidance of physical information. We adopt the diffusion process proposed in DDPM [18] to construct the PDT branch, which can be described as a forward diffusion process and a reverse diffusion process.

Forward Diffusion Process. The forward diffusion process can be viewed as a Markov chain progressively adding Gaussian noise to the data. Given a clean data x_0 , then introduce Gaussian noise based on the time step, as follows:

$$q(x_t|x_{t-1}) = \mathcal{N}(x_t; \sqrt{1 - \beta_t}x_{t-1}, \beta_t I), \quad (1)$$

where β_t is a variable controlling the variance of the noise. Introducing $\alpha_t = 1 - \beta_t$, this process can be described as:

$$x_t = \sqrt{\alpha_t}x_{t-1} + \sqrt{1 - \alpha_t}\epsilon_{t-1}, \quad \epsilon_{t-1} \sim \mathcal{N}(0, \mathcal{Z}). \quad (2)$$

With Gaussian distributions are merged, We can obtain :

$$q(x_t|x_0) = \mathcal{N}(x_t; \sqrt{\alpha_t}x_0, (1 - \alpha_t)I). \quad (3)$$

Reverse Diffusion Process. The reverse diffusion process aims to restore the clean data from the Gaussian noise. The reverse diffusion can be expressed as:

$$p_\theta(x_{t-1}|x_t, x_c) = \mathcal{N}(x_{t-1}; \mu_\theta(x_t, x_c, t), \sigma_t^2 \mathcal{Z}), \quad (4)$$

where x_c refers to the conditional image I (underwater input image). $\mu_\theta(x_t, x_c, t)$ and σ_t^2 are the mean and variance from the estimate of step t , respectively. We follow the setup of [18], they can be expressed as:

$$\mu_\theta(x_t, x_c, t) = \frac{1}{\sqrt{\alpha_t}} \left(x_t - \frac{\beta_t}{(1 - \alpha_t)} \epsilon_\theta(x_t, x_c, t) \right), \quad (5)$$

$$\sigma_t^2 = \frac{1 - \bar{\alpha}_{t-1}}{1 - \bar{\alpha}_t} \beta_t, \quad (6)$$

where $\epsilon_\theta(x_t, x_c, t)$ is the estimated value with a Unet.

We optimize an objective function for the noise estimated by the network and the noise ϵ actually added. Therefore, the diffusion loss is:

$$L_{dm}(\theta) = \|\epsilon - \epsilon_\theta(\sqrt{\alpha_t}x_0 + \sqrt{1 - \alpha_t}\epsilon, x_c, t)\|. \quad (7)$$

3.2 Physics Prior Generation

Mathematically, the underwater images can be expressed by the modified Koschmieder light scanning model [1]:

$$I^c(x) = J^c(x)T^c(x) + (1 - T^c(x))B^c, \quad (8)$$

where $c \in \{R, G, B\}$ is the color channel, x indicates the spatial location of each pixel, I^c is the observed underwater image, J^c is the restored clean image, T^c is the medium transmission map, and B^c is the global background scattered light. In Physics Prior Generation (PPG) branch, our goal is to produce T^c and B^c from the underwater image I^c , exploiting the physics model.

Network architecture of PPG branch is shown in Fig. 1, and consists of two sub-networks: transmission map generation sub-network $\mathcal{T}(x)$ and background light generation sub-network $\mathcal{B}(x)$. The two sub-networks consist of duplicated Dynamic Convolutions (DC) [7]. DC dynamically combines numerous parallel convolutional kernels according to their attention, thereby enhancing the model's complexity and performance without augmenting the network's depth or breadth. Given that the background light differs fundamentally from the transmission map, being independent of image content and instead encapsulating the global properties [15], for the purpose of generating the background light component, our background light generation sub-network initially employs a Gaussian blur block (GBB) to eliminate fine-grained content details and thereby extract the inherent global attributes.

Given a underwater image as input I and its corresponding ground truth (GT), we can obtain via Eq. 8:

$$\hat{I} = GT \cdot \mathcal{T}(I) + (1 - \mathcal{T}(I))\mathcal{B}(GBB(I)), \quad (9)$$

We constrain the PPG branch by supervised manner. The physics reconstruction loss of PPG branch can be expressed as:

$$\mathcal{L}_p = \|\hat{I} - I\|_1. \quad (10)$$

To enhance the perceptual similarity of the reconstructed images, we introduce the perceptual Loss \mathcal{L}_{per} :

$$\mathcal{L}_{per} = \|\phi(\hat{I}) - \phi(I)\|_2, \quad (11)$$

where ϕ is a pre-trained VGG network.

Finally, the overall loss \mathcal{L}_{ppg} of PPG branch can be expressed as:

$$\mathcal{L}_{ppg} = \lambda_1 \mathcal{L}_p + \lambda_2 \mathcal{L}_{per}. \quad (12)$$

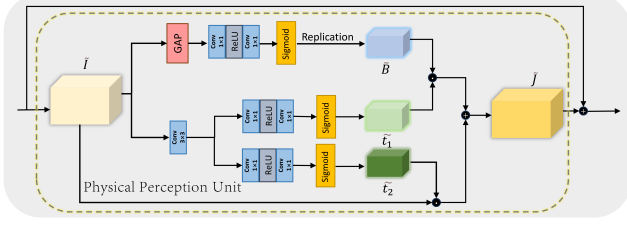


Figure 3: The detailed structure of the proposed physics perception unit (PPU).

3.3 Implicit Neural Reconstruction

Inspired by [6, 37, 50] based on implicit neural representations that can encode an image as a continuous function and learn a more robust feature representation, we further introduce Implicit Neural Representations (INRs) to learn robust degradation representations from diverse underwater image, aiming to reduce the difficulty of restoration for diffusion models. INRs trains a multi-layer perceptron (MLP) by learning the following mapping :

$$F_{\theta} : \mathbb{R}^2 \rightarrow \mathbb{R}^3, \quad (13)$$

where the dimensions of input refer to the (x, y) spatial coordinates, while the dimensions of output refer to the (R, G, B) color channels. Specifically, following the setting of [6, 50], underwater image I is transformed to a feature map $\mathbf{E} \in \mathbb{R}^{H \times W \times C}$ with a image resolution of $H \times W$. Meanwhile, the position of each pixel is recorded in a relative coordinate set $\mathbf{X} \in \mathbb{R}^{H \times W \times 2}$, where the value '2' means horizontal and vertical coordinates. As shown in Figure 1, we fuse \mathbf{X} and \mathbf{E} , and use F_{θ} to output image I_{inr} , which is expressed as:

$$I_{\text{inr}}[x, y] = F_{\theta}(\mathbf{E}[x, y], \mathbf{X}[x, y]), \quad (14)$$

where $[x, y]$ is the location of a pixel and $I_{\text{inr}}[x, y]$ is the generated RGB value. Due to the elimination of high-frequency components during rendering [50], we adopt periodic spatial encoding [22] to project the pixel coordinates \mathbf{X} into a higher dimensional space \mathbb{R}^{2L} for better recovering high-frequency details. The encoding procedure is formulated as:

$$\mathbf{X}' = \gamma(\mathbf{X}), \quad (15)$$

$$\gamma(c) = (\dots, \sin(2^i c), \cos(2^i c), \dots), \quad (16)$$

where $\gamma()$ represents a spatial encoding function. i values from 0 to $L-1$, $c \in \mathbb{R}^{2L}$ is the coordinate value of \mathbf{X} , and L is a hyperparameter that determines the dimension value. Given a GT of underwater image GT , The reconstruction loss of INR branch can be expressed as:

$$\mathcal{L}_{\text{INR}} = \|I_{\text{inr}} - GT\|_1. \quad (17)$$

Finally, we fuse I and I_{inr} to obtain the condition x_c of diffusion model, which can be expressed as:

$$x_c = I_{\text{inr}} + I. \quad (18)$$

3.4 Physics-aware Diffusion Transformer

Physics-aware diffusion transformer (PDT) branch aims to exploit the extracted physics prior information from PPG branch for better guiding underwater image restoration. Fig. 1 shows the overall of PDT branch, which is a U-shaped structure with physics-aware

diffusion transformer (PDT) blocks and cross attention module (CAM).

Given the output of the INR branch as condition image $x_c \in \mathbb{R}^{H \times W \times 3}$ and the background light $B^c \in \mathbb{R}^{H \times W \times 3}$ as a physical prior condition, we first obtain the noise sample $x_t \in \mathbb{R}^{H \times W \times 3}$ at time step t according to the forward process, and concatenate x_t , B^c and x_c at channel dimension to obtain the input of PDT branch. Then, we obtain the embedding features $\mathbf{F} \in \mathbb{R}^{H \times W \times C}$ through convolution, where C means the number of channel. \mathbf{F} is encoded and decoded by PDT block, which consists of physics-aware self-attention (PA-SA), physics perception unit and gated multi-scale feed-forward network (GM-FFN). Note that, we introduce a physics perception unit (PPU) to further exploit the beneficial feature-level physics information.

Cross Attention Module. CAM aims to obtain a physics-aware interaction embedding, using which guides the diffusion process. We denote T^c and \mathbf{F} as the input of CAM. We use different linear projections to construct Q and K in CAM:

$$Q = \text{Conv}_{1 \times 1}(T^c), \quad (19)$$

$$K = \text{Conv}_{1 \times 1}(\mathbf{F}). \quad (20)$$

Similarly, V of the transmission map T^c can be obtained:

$$V = \text{Conv}_{1 \times 1}(T^c). \quad (21)$$

The output feature map of CAM T_{out} can then be obtained from the formula:

$$T_{\text{out}} = \text{Softmax}\left(\frac{QK^T}{\sqrt{d_k}}\right)V. \quad (22)$$

Physics-aware Self-attention. As is shown in Figure 2 (a), we first embed the time embedding \mathbf{t} into the input features \mathbf{F} in our PA-SA:

$$\tilde{\mathbf{F}} = \text{Norm}(\mathbf{F}) + \mathbf{t}, \quad (23)$$

where Norm means layer normalization. We first obtain query ($Q_f = \mathbf{W}_d \mathbf{W}_p \tilde{\mathbf{F}}$), key ($K = \mathbf{W}_d \mathbf{W}_p \tilde{\mathbf{F}}$), and value ($V = \mathbf{W}_d \mathbf{W}_p \tilde{\mathbf{F}}$) from the embedding input features \mathbf{F} . Meanwhile, we generate query ($Q_t = \mathbf{W}_d \mathbf{W}_p T_{\text{out}}$) from the output feature map of CAM, where \mathbf{W}_p and \mathbf{W}_d respectively denote 1×1 point-wise convolution and 3×3 depth-wise convolution. We employ physics-aware query-driven attention strategy to obtain the final query Q by fusing Q_t and Q_f , which can be expressed as:

$$Q = \text{Conv}_{1 \times 1}(\text{concat}(Q_f, Q_t)). \quad (24)$$

We employ self-attention and get the output of PA-SA $\hat{\mathbf{F}}$:

$$\hat{\mathbf{F}} = \mathbf{F} + \text{softmax}\left(\frac{QK^T}{\alpha}\right) \cdot V, \quad (25)$$

where α is a learnable parameter. Consequently, PA-SA introduces physical guidance to fully exploit physics knowledge at the feature level and use self-attention mechanism to implicitly model the features of transmission map, which can help the diffusion model restore missing details and correct color distortion.

Physics Perception Unit. Exploring feature-level physics information [12, 59] achieved success in image dehazing tasks. Our proposed physics perception unit (PPU) aims to further exploit the beneficial feature-level physics information for underwater image enhancement, and learn richer physical features. Our proposed PPU is based on the simplified atmospheric model Eq. (8), as shown in

Fig. 3. We can reformulate the physics model to represent the clear image J , which can be obtained by:

$$J^c(\mathbf{x}) = I^c(\mathbf{x}) \frac{1}{T^c(\mathbf{x})} + B^c \left(1 - \frac{1}{T^c(\mathbf{x})}\right). \quad (26)$$

Let k denote a feature extractor (the filter kernel in a deep network). Then extracting features via the feature extractor k , Eq. (25) can be reformulated as follows:

$$k \otimes J = k \otimes \left(I \odot \frac{1}{t}\right) + k \otimes B \left(1 - \frac{1}{t}\right), \quad (27)$$

where \otimes denotes the convolution operator and \odot denotes the element-wise product operation. Using the matrix-vector form for algebraic operations, Eq. (26) can be expressed as:

$$KJ = KT_1I + KT_2B, \quad (28)$$

where K, J, I, B, T_1 and T_2 respectively denote the matrix-vector forms of $k, J, I, B, \frac{1}{t}$ and $(1 - \frac{1}{t})$. Note that the diagonal vector of the diagonal matrix T_1 corresponds to the vectorized form of $\frac{1}{t}$. Assuming that K is an invertible matrix-vector, we can obtain

$$F_1 = KT_1K^{-1}, \quad (29)$$

$$F_2 = KT_2K^{-1}. \quad (30)$$

And then, Eq. (27) can be expressed as:

$$\begin{aligned} KJ &= (KT_1K^{-1})KI + (KT_2K^{-1})KB \\ &= F_1(KI) + F_2(KB). \end{aligned} \quad (31)$$

The Eq. (30) presents the relation between the clear image and the underwater image in a deep feature space. Due to the strong representation ability of deep neural networks, we can design a feature-level physics perception unit (PPU) and adopt deep networks to approximate the features corresponding to F_1, F_2 and KB . We denote \tilde{B} as an approximation of the features KB that correspond to the background light, and \tilde{t}_1 and \tilde{t}_2 as approximations of F_1 and F_2 , which are associated with the transmission map. Furthermore, KI and KJ can be viewed as a latent underwater image \tilde{I} and its corresponding latent clear image \tilde{J} , respectively. According to Eq. (30), the \tilde{J} can be expressed as:

$$\tilde{J} = \tilde{t}_1 \odot \tilde{I} + \tilde{t}_2 \odot \tilde{B}. \quad (32)$$

Since the background light is usually assumed to be homogeneous, we can use global average pooling (GAP) to obtain the main information for \tilde{B} in the feature space. \tilde{B} can be expressed:

$$\tilde{B} = H(\sigma(\text{Conv}(\text{ReLU}(\text{Conv}(\text{GAP}(\tilde{I})))))), \quad (33)$$

where σ is the Sigmoid function, H denotes a replication operation.

As the transmission map is non-homogeneous, we cannot apply GAP for the approximations of \tilde{t}_1 and \tilde{t}_2 . We use different projection networks to obtain \tilde{t}_1 and \tilde{t}_2 :

$$\tilde{t}_1 = \sigma(\text{Conv}(\text{ReLU}(\text{Conv}(\text{Conv}_s(\tilde{I}))))), \quad (34)$$

$$\tilde{t}_2 = \sigma(\text{Conv}(\text{ReLU}(\text{Conv}(\text{Conv}_s(\tilde{I}))))). \quad (35)$$

where s represents the shared Conv layer. Given \hat{F} as the input of PPU, we use residual connection to obtain the final output of PPU, which can be expressed as:

$$F_{\text{ppu}} = \text{PPU}(\hat{F}) + \hat{F}. \quad (36)$$

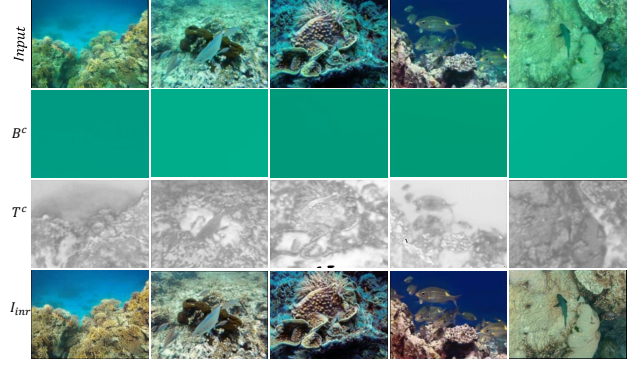


Figure 4: The visual results of the background scattered light B^c , the medium transmission map $T^c(x)$, and the implicit neural output I_{inr} .

Gated Multi-scale Feed-Forward Network. Finally, we design a GM-FFN for local feature aggregation. As is shown in Figure 2 (b), we employ GD-FFN-like structure [55] to construct our feed-forward network. In order to expand the receptive field, we employ multi-scale kernel depth-wise convolutions. GM-FFN adopts GELU to ensure the flexibility of feature aggregation.

4 EXPERIMENTS

4.1 Experimental Settings

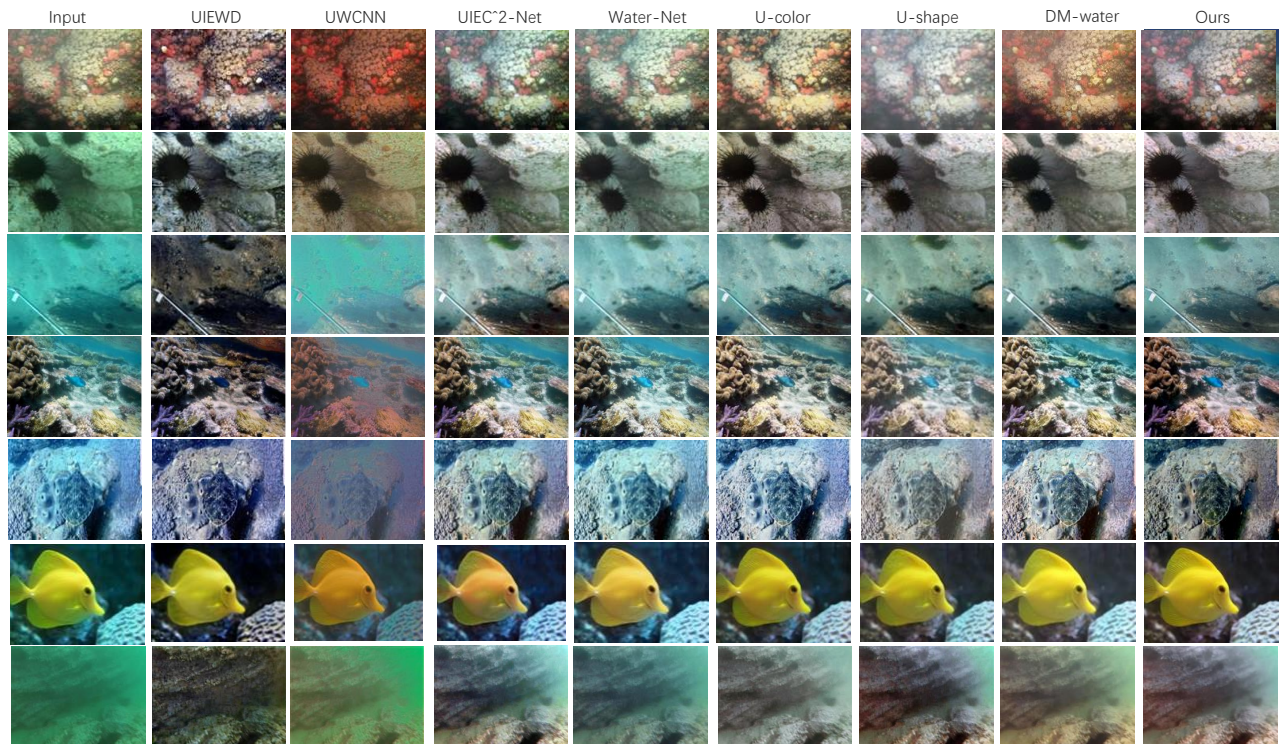
Implementation details. Our network, implemented using PyTorch 1.7, underwent training and testing on an NVIDIA GeForce RTX 3090 GPU. We employed the Adam optimizer with $\beta_1 = 0.9$ and $\beta_2 = 0.999$. The learning rate was established at 0.0001. During the training stage, to balance the batch size and image size, the batch and image size are set to 2 and 256×256 , respectively. The number of training iterations reached one million. The pixel values of the image are normalized to $[-1, 1]$. The time step of the diffusion model is set to 2000. In the testing stage, following the setting in [44], the input size of the image is 256×256 . By using the skip sampling strategy, and the sampling times are set to 10 times to balance the performance and runtime.

Datasets. We utilize the real-world UIEBD dataset [34] and the LSUI dataset [24] for training and evaluating our model. The UIEBD dataset comprises 890 underwater images with corresponding labels. Out of these, 700 images are allocated for training, and the remaining 190 are designated for testing. LSUI dataset contains 5004 underwater images and their corresponding high-quality images. Compared with UIEBD, LSUI contains diverse underwater scenes, object categories and deep-sea and cave images. In the paper, The LSUI dataset is randomly partitioned into 4500 images for training and 504 images for testing. In addition, to verify the generalization of PA-Diff, we use non-reference benchmarks U45 [25], which contains 45 underwater images for testing.

Comparison methods. We conduct a comparative analysis between PA-Diff and seven state-of-the-art (SOTA) UIE methods, namely UIEC²-Net [45], Water-Net [34], UWCNN [4], UIEWD [28], U-color [23], U-shape [24], and DM-water [44]. To ensure a fair and rigorous comparison, we utilize the provided source codes

Table 1: Quantitative comparison on the UIEBD and LSUI datasets. The best results are highlighted in bold and the second best results are underlined.

	Methods	UIEWD	UWCNN	UIEC ² -Net	Water-Net	U-color	U-shape	DM-water	Ours
UIEBD	FID↓	85.12	94.44	35.06	37.48	38.25	46.11	<u>31.07</u>	28.74
	LPIPS↓	0.3956	0.3525	0.2033	0.2116	0.2337	0.2264	<u>0.1436</u>	0.1328
	PSNR↑	14.65	15.40	20.14	19.35	20.71	21.25	21.88	<u>21.56</u>
	SSIM↑	0.7265	0.7749	0.8215	0.8321	0.8411	<u>0.8453</u>	0.8194	0.8642
LSUI	FID↓	98.49	100.5	34.51	38.90	45.06	28.56	<u>27.91</u>	22.13
	LPIPS↓	0.3962	0.3450	0.1432	0.1678	0.123	<u>0.1028</u>	0.1138	0.0922
	PSNR↑	15.43	18.24	20.86	19.73	22.91	24.16	<u>27.65</u>	27.77
	SSIM↑	0.7802	0.8465	0.8867	0.8226	0.8902	<u>0.9322</u>	0.8867	0.9378
U45	UIQM↑	2.458	2.379	2.780	2.957	3.104	<u>3.151</u>	3.086	3.147
	UCIQE↑	0.583	0.567	0.591	0.601	0.586	0.592	<u>0.634</u>	0.653

**Figure 5: Qualitative comparison with other SOTA methods on the UIEBD and LSUI datasets.**

from the respective authors and adhere strictly to the identical experimental settings across all evaluations.

Evaluation Metrics. We employ standard full-reference image quality assessment metrics, including PSNR and SSIM [48], for quantitative comparisons at both pixel and structural levels. Higher PSNR and SSIM values indicate superior image quality. Additionally, LPIPS [56] and FID [17] are utilized to evaluate perceptual performance. Lower LPIPS and FID scores signify a more effective UIE approach. For non-reference benchmarks U45, we introduce UIQM [33] and UCIQE [49] to evaluate our method.

4.2 Results and Comparisons

Table 1 shows the quantitative results compared with different SOTA methods on the UIEBD, LSUI and U45 datasets, including with UIEC²-Net [45], Water-Net [34], UIEWD [28], UWCNN [4], U-color [23], U-shape [24], and DM-water [44]. We mainly use PSNR, SSIM, LPIPS and FID as our quantitative indices for UIEBD and LSUI datasets, and UIQM and UCIQE for non-reference dataset U45. The results in Table 1 show that our algorithm outperforms state-of-the-art methods obviously, especially in terms of perceptual metrics. To better validate the superiority of our methods, Fig. 5 shows the visual comparison results with other methods on the UIEBD and

Table 2: Ablation study on LSUI dataset. T^c and B^c refer to transmission map and background light prior information in PPG branch, respectively. GBB means Gaussian blur module. INR represents our INR branch. PSE refers to the periodic spatial encoding [22], aiming to better recover high-frequency details. CAM and PPU means our designed cross attention module and physics perception unit, respectively. $GM - FFN$ means multi-scale operation in the feed-forward network.

Method	B^c	T^c	GBB	INR	PSE	CAM	PPU	$GM - FFN$	$GD - FFN$ [55]	FID↓	SSIM↑
A	×	×	×	×	×	×	×	×	✓	28.35	0.8893
B	✓	×	×	×	×	×	×	×	✓	27.71	0.8974
C	✓	✓	×	×	×	×	×	×	✓	25.92	0.9071
D	✓	✓	✓	×	×	×	×	×	✓	25.24	0.9112
E	✓	✓	✓	✓	×	×	×	×	✓	24.50	0.9186
F	✓	✓	✓	✓	✓	×	×	×	✓	24.92	0.9176
G	✓	✓	✓	✓	✓	✓	×	×	✓	23.66	0.9241
H	✓	✓	✓	✓	✓	✓	✓	×	✓	22.85	0.9374
Ours	✓	✓	✓	✓	✓	✓	✓	✓	×	22.13	0.9378

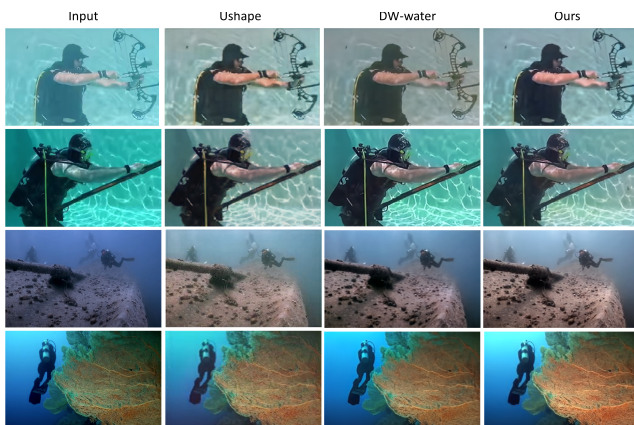


Figure 6: More visual results from real-world scenarios.

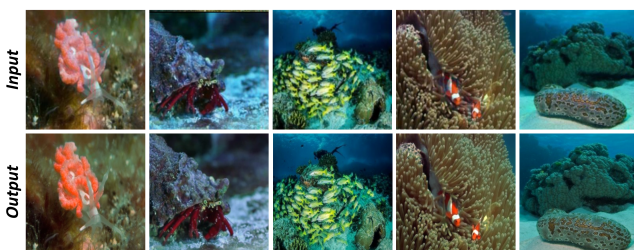


Figure 7: Limitations. The output images refer to the reconstruction images of PPG branch.

LSUI datasets. The some examples are randomly selected on the UIEBD and LSUI datasets. Furthermore, in order to more effectively validate the generalization performance of our method on real-world images, we present enhancement results from real scenes in Figure 6. Our methods consistently generate natural and better visual results, strongly proving that PA-Diff has good generalization performance for real-world underwater images.

4.3 Ablation Study

To evaluate the impact of each strategy on the diffusion model, we conduct a comprehensive ablation study. Table 2 shows the ablation results on the LSUI dataset. We use a full-reference assessment metric (SSIM) and perceptual assessment metric (FID) to evaluate the ablation study, respectively. Model A means that we just employ the most basic diffusion transformer structure. Firstly, we investigate the influence of the PPG branch on the diffusion process. Compared with model A, model B, C and D achieve better results, suggesting that the prior knowledge of physics can help diffusion model to better restore image. Particularly, Model B exhibits a remarkable advancement in terms of PSNR metric, suggesting that the transmission map T^c plays a highly effective role in guiding the diffusion process. Model D outperforms C, suggesting that GBB is also useful to exploit more helpful the background light information for the diffusion process. Subsequently, we explore the impact of the INR branch on the performance of the diffusion model. Model E outperforms D, suggesting that INR branch can improve the performance and reduce the difficulty of restoration for diffusion models. Model F outperforms E, implying that the periodic spatial encoding can enhance the representation ability of INR branch. Subsequently, for models G and H, we respectively delve into the effects of our designed CAM and PPU on the model performance. Both models G and H yield improved outcomes, proving the significant role that CAM and PPU play in extracting more valuable feature-level physical information. Finally, Ours achieves the best performance, proving that our all contribution is effective for UIE tasks. Moreover, we also examine the applicability of PPU in other baseline models. Table 3 showcases the adaptability of PPU across different UIE methods, demonstrating its generalizability potential to exploit the beneficial feature-level physics information.

Limitations. As illustrated in Figure 7, there remains a discernible discrepancy between the reconstructed images from the PPG branch and the corresponding input images, indicating an existing gap between the physical information generated by our PPG branch and the ideal or ground-truth physical representation.

Table 3: Ablation study with the PPU on UIEBD.

Method	Unet	DW-water	Ushape
w/o PPU(PSNR/SSIM)	17.41/0.7769	21.88/0.8194	21.25/0.8453
w PPU(PSNR/SSIM)	19.64/0.8157	21.23/0.8331	21.89/0.8570

Consequently, how to generate more accurate a prior knowledge of physics remains a problem we need to research in the future.

5 CONCLUSION

In this paper, we develop a novel UIE framework, namely PA-Diff. With utilizing physics prior information to guide the diffusion process, PA-Diff can obtain underwater-aware ability and model the complex distribution in real-world underwater scenes. To the best of our knowledge, it is the first the diffusion model based on physical perception in image enhancement tasks. Our designed PPU is a plug-and-play universal module to exploit the beneficial feature-level physics information, which can be integrated into any deep learning network. PA-Diff shows SOTA performance on UIE task, and extensive ablation experiments can prove that each of our contributions is effective.

REFERENCES

- [1] Derya Akkaynak and Tali Treibitz. 2019. Sea-thru: A method for removing water from underwater images. In *Proceedings of the IEEE/CVF conference on computer vision and pattern recognition*. 1682–1691.
- [2] Derya Akkaynak and Tali Treibitz. 2019. Sea-Thru: A Method for Removing Water From Underwater Images. In *IEEE Conference on Computer Vision and Pattern Recognition, CVPR 2019, Long Beach, CA, USA, June 16–20, 2019*. Computer Vision Foundation / IEEE, 1682–1691.
- [3] Derya Akkaynak, Tali Treibitz, Tom Shlesinger, Yossi Loya, Raz Tamir, and David Iluz. 2017. What is the Space of Attenuation Coefficients in Underwater Computer Vision?. In *2017 IEEE Conference on Computer Vision and Pattern Recognition, CVPR 2017, Honolulu, HI, USA, July 21–26, 2017*. 568–577.
- [4] Saeed Anwar, Chongyi Li, and Fatih Porikli. 2018. Deep Underwater Image Enhancement. *CoRR abs/1807.03528* (2018). arXiv:1807.03528
- [5] Hao-Wei Chen, Yu-Syuan Xu, Min-Fong Hong, Yi-Min Tsai, Hsien-Kai Kuo, and Chun-Yi Lee. 2023. Cascaded local implicit transformer for arbitrary-scale super-resolution. In *Proceedings of the IEEE/CVF Conference on Computer Vision and Pattern Recognition*. 18257–18267.
- [6] Xiang Chen, Jinshan Pan, and Jiangxin Dong. 2024. Bidirectional Multi-Scale Implicit Neural Representations for Image Deraining. In *Proceedings of the IEEE/CVF Conference on Computer Vision and Pattern Recognition (CVPR)*.
- [7] Yinpeng Chen, Xiyang Dai, Mengchen Liu, Dongdong Chen, Lu Yuan, and Zicheng Liu. 2020. Dynamic convolution: Attention over convolution kernels. In *Proceedings of the IEEE/CVF conference on computer vision and pattern recognition*. 11030–11039.
- [8] Yinbo Chen, Sifei Liu, and Xiaolong Wang. 2021. Learning continuous image representation with local implicit image function. In *Proceedings of the IEEE/CVF conference on computer vision and pattern recognition*. 8628–8638.
- [9] John Yi-Wu Chiang and Ying-Ching Chen. 2012. Underwater Image Enhancement by Wavelength Compensation and Dehazing. *IEEE Trans. Image Process.* 21, 4 (2012), 1756–1769.
- [10] Jooyoung Choi, Sungwon Kim, Yonghyun Jeong, Youngjune Gwon, and Sungroh Yoon. 2021. ILVR: Conditioning Method for Denoising Diffusion Probabilistic Models. In *2021 IEEE/CVF International Conference on Computer Vision, ICCV 2021, Montreal, QC, Canada, October 10–17, 2021*. IEEE, 14347–14356.
- [11] Karin de Langis and Junaed Sattar. 2020. Realtime Multi-Diver Tracking and Re-identification for Underwater Human-Robot Collaboration. In *2020 IEEE International Conference on Robotics and Automation, ICRA 2020, Paris, France, May 31 - August 31, 2020*. 11140–11146.
- [12] Jiangxin Dong and Jinshan Pan. 2020. Physics-based feature dehazing networks. In *Computer Vision—ECCV 2020: 16th European Conference, Glasgow, UK, August 23–28, 2020, Proceedings, Part XXX 16*. Springer, 188–204.
- [13] Dazhao Du, Enhao Li, Lingyu Si, Fanjiang Xu, Jianwei Niu, and Fuchun Sun. 2023. UIEDP: Underwater Image Enhancement with Diffusion Prior. *arXiv preprint arXiv:2312.06240* (2023).
- [14] Cameron Fabbri, Md Jahidul Islam, and Junaed Sattar. 2018. Enhancing Underwater Imagery Using Generative Adversarial Networks. In *2018 IEEE International Conference on Robotics and Automation, ICRA 2018, Brisbane, Australia, May 21–25, 2018*. IEEE, 7159–7165.
- [15] Zhenqi Fu, Huangxing Lin, Yan Yang, Shu Chai, Liyan Sun, Yue Huang, and Xinghao Ding. 2022. Unsupervised underwater image restoration: From a homology perspective. In *Proceedings of the AAAI Conference on Artificial Intelligence*, Vol. 36. 643–651.
- [16] Zhenqi Fu, Wu Wang, Yue Huang, Xinghao Ding, and Kai-Kuang Ma. 2022. Uncertainty inspired underwater image enhancement. In *European conference on computer vision*. Springer, 465–482.
- [17] Martin Heusel, Hubert Ramsauer, Thomas Unterthiner, Bernhard Nessler, and Sepp Hochreiter. 2017. GANs Trained by a Two Time-Scale Update Rule Converge to a Local Nash Equilibrium. In *Advances in Neural Information Processing Systems 30: Annual Conference on Neural Information Processing Systems 2017, December 4–9, 2017, Long Beach, CA, USA*. 6626–6637.
- [18] Jonathan Ho, Ajay Jain, and Pieter Abbeel. 2020. Denoising Diffusion Probabilistic Models. In *Advances in Neural Information Processing Systems 33: Annual Conference on Neural Information Processing Systems 2020, NeurIPS 2020, December 6–12, 2020, virtual*.
- [19] Qun Jiang, Yunfeng Zhang, Fangxun Bao, Xiuyang Zhao, Caiming Zhang, and Peide Liu. 2022. Two-step domain adaptation for underwater image enhancement. *Pattern Recognition* 122 (2022), 108324.
- [20] Paulo Drews Jr., Erickson Rangel do Nascimento, F. Moraes, Silvia S. C. Botelho, and Mario F. M. Campos. 2013. Transmission Estimation in Underwater Single Images. In *2013 IEEE International Conference on Computer Vision Workshops, ICCV Workshops 2013, Sydney, Australia, December 1–8, 2013*. 825–830.
- [21] Jaewon Lee, Kwang Pyo Choi, and Kyong Hwan Jin. 2022. Learning local implicit fourier representation for image warping. In *European Conference on Computer Vision*. Springer, 182–200.
- [22] Jaewon Lee and Kyong Hwan Jin. 2022. Local texture estimator for implicit representation function. In *Proceedings of the IEEE/CVF conference on computer vision and pattern recognition*. 1929–1938.
- [23] Chongyi Li, Saeed Anwar, Junhui Hou, Runmin Cong, Chunle Guo, and Wenqi Ren. 2021. Underwater Image Enhancement via Medium Transmission-Guided Multi-Color Space Embedding. *IEEE Trans. Image Process.* 30 (2021), 4985–5000.
- [24] Chongyi Li, Chunle Guo, Wenqi Ren, Runmin Cong, Junhui Hou, Sam Kwong, and Dacheng Tao. 2020. An Underwater Image Enhancement Benchmark Dataset and Beyond. *IEEE Trans. Image Process.* 29 (2020), 4376–4389.
- [25] Hanyu Li, Jingjing Li, and Wei Wang. 2019. A fusion adversarial underwater image enhancement network with a public test dataset. *arXiv preprint arXiv:1906.06819* (2019).
- [26] Shilin Lu, Yanzhu Liu, and Adams Wai-Kin Kong. 2023. Tf-icon: Diffusion-based training-free cross-domain image composition. In *Proceedings of the IEEE/CVF International Conference on Computer Vision*. 2294–2305.
- [27] Shilin Lu, Zilan Wang, Leyang Li, Yanzhu Liu, and Adams Wai-Kin Kong. 2024. MACE: Mass Concept Erasure in Diffusion Models. *arXiv preprint arXiv:2403.06135* (2024).
- [28] Ziyin Ma and Changjae Oh. 2022. A Wavelet-Based Dual-Stream Network for Underwater Image Enhancement. In *IEEE International Conference on Acoustics, Speech and Signal Processing, ICASSP 2022, Virtual and Singapore, 23–27 May 2022*. IEEE, 2769–2773.
- [29] James McMahon and Erion Plaku. 2021. Autonomous Data Collection With Timed Communication Constraints for Unmanned Underwater Vehicles. *IEEE Robotics Autom. Lett.* 6, 2 (2021), 1832–1839.
- [30] Pan Mu, Jing Fang, Haotian Qian, and Cong Bai. 2023. Transmission and Color-guided Network for Underwater Image Enhancement. In *2023 IEEE International Conference on Multimedia and Expo (ICME)*. IEEE, 1337–1342.
- [31] Pan Mu, Hanning Xu, Zheyuan Liu, Zheng Wang, Sixian Chan, and Cong Bai. 2023. A generalized physical-knowledge-guided dynamic model for underwater image enhancement. In *Proceedings of the 31st ACM International Conference on Multimedia*. 7111–7120.
- [32] Ozan Özdenizci and Robert Legenstein. 2023. Restoring vision in adverse weather conditions with patch-based denoising diffusion models. *IEEE Transactions on Pattern Analysis and Machine Intelligence* (2023).
- [33] Karen Panetta, Chen Gao, and Sos Agaian. 2015. Human-visual-system-inspired underwater image quality measures. *IEEE Journal of Oceanic Engineering* 41, 3 (2015), 541–551.
- [34] Lintao Peng, Chunli Zhu, and Liheng Bian. 2023. U-Shape Transformer for Underwater Image Enhancement. *IEEE Trans. Image Process.* 32 (2023), 3066–3079.
- [35] Yan-Tsung Peng, Keming Cao, and Pamela C. Cosman. 2018. Generalization of the Dark Channel Prior for Single Image Restoration. *IEEE Trans. Image Process.* 27, 6 (2018), 2856–2868.
- [36] Yan-Tsung Peng and Pamela C. Cosman. 2017. Underwater Image Restoration Based on Image Blurriness and Light Absorption. *IEEE Trans. Image Process.* 26, 4 (2017), 1579–1594.
- [37] Yuhui Quan, Xin Yao, and Hui Ji. 2023. Single Image Defocus Deblurring via Implicit Neural Inverse Kernels. In *Proceedings of the IEEE/CVF International Conference on Computer Vision*. 12600–12610.

- [38] Robin Rombach, Andreas Blattmann, Dominik Lorenz, Patrick Esser, and Björn Ommer. 2022. High-Resolution Image Synthesis with Latent Diffusion Models. In *IEEE/CVF Conference on Computer Vision and Pattern Recognition, CVPR 2022, New Orleans, LA, USA, June 18-24, 2022*. IEEE, 10674–10685.
- [39] Chitwan Saharia, William Chan, Huiwen Chang, Chris A. Lee, Jonathan Ho, Tim Salimans, David J. Fleet, and Mohammad Norouzi. 2022. Palette: Image-to-Image Diffusion Models. In *SIGGRAPH '22: Special Interest Group on Computer Graphics and Interactive Techniques Conference, Vancouver, BC, Canada, August 7 - 11, 2022*. ACM, 15:1–15:10.
- [40] Chitwan Saharia, William Chan, Saurabh Saxena, Lala Li, Jay Whang, Emily L. Denton, Seyed Kamyar Seyed Ghasemipour, Raphael Gontijo Lopes, Burcu Karagol Ayan, Tim Salimans, Jonathan Ho, David J. Fleet, and Mohammad Norouzi. 2022. Photorealistic Text-to-Image Diffusion Models with Deep Language Understanding. In *NeurIPS*.
- [41] Jiaming Song, Chenlin Meng, and Stefano Ermon. 2021. Denoising Diffusion Implicit Models. In *9th International Conference on Learning Representations, ICLR 2021, Virtual Event, Austria, May 3-7, 2021*.
- [42] Yannick Strümpfer, Janis Postels, Ren Yang, Luc Van Gool, and Federico Tombari. 2022. Implicit neural representations for image compression. In *European Conference on Computer Vision*. Springer, 74–91.
- [43] Yu Sun, Jiaming Liu, Mingyang Xie, Brendt Wohlberg, and Ulugbek S Kamilov. 2021. Coil: Coordinate-based internal learning for imaging inverse problems. *arXiv preprint arXiv:2102.05181* (2021).
- [44] Yi Tang, Hiroshi Kawasaki, and Takafumi Iwaguchi. 2023. Underwater Image Enhancement by Transformer-based Diffusion Model with Non-uniform Sampling for Skip Strategy. In *Proceedings of the 31st ACM International Conference on Multimedia, MM 2023, Ottawa, ON, Canada, 29 October 2023- 3 November 2023*. ACM, 5419–5427.
- [45] Yudong Wang, Jichang Guo, Huan Gao, and Huihui Yue. 2021. UIEC²-Net: CNN-based underwater image enhancement using two color space. *Signal Process. Image Commun.* 96 (2021), 116250.
- [46] Yi Wang, Hui Liu, and Lap-Pui Chau. 2018. Single Underwater Image Restoration Using Adaptive Attenuation-Curve Prior. *IEEE Trans. Circuits Syst. I Regul. Pap.* 65-1, 3 (2018), 992–1002.
- [47] Yinhuai Wang, Jiwen Yu, and Jian Zhang. 2023. Zero-Shot Image Restoration Using Denoising Diffusion Null-Space Model. In *The Eleventh International Conference on Learning Representations, ICLR 2023, Kigali, Rwanda, May 1-5, 2023*.
- [48] Zhou Wang, Alan C. Bovik, Hamid R. Sheikh, and Eero P. Simoncelli. 2004. Image quality assessment: from error visibility to structural similarity. *IEEE Trans. Image Process.* 13, 4 (2004), 600–612.
- [49] Miao Yang and Arcot Sowmya. 2015. An underwater color image quality evaluation metric. *IEEE Transactions on Image Processing* 24, 12 (2015), 6062–6071.
- [50] Shuzhou Yang, Moxuan Ding, Yanmin Wu, Zihan Li, and Jian Zhang. 2023. Implicit neural representation for cooperative low-light image enhancement. In *Proceedings of the IEEE/CVF International Conference on Computer Vision*. 12918–12927.
- [51] Shuzhou Yang, Xuanyu Zhang, Yinhuai Wang, Jiwen Yu, Yuhan Wang, and Jian Zhang. 2023. DiffLLE: Diffusion-guided Domain Calibration for Unsupervised Low-light Image Enhancement. *arXiv preprint arXiv:2308.09279* (2023).
- [52] Zongyuan Yang, Baolin Liu, Yongping Xiong, Lan Yi, Guibin Wu, Xiaojun Tang, Ziqi Liu, Junjie Zhou, and Xing Zhang. 2023. DocDiff: Document enhancement via residual diffusion models. In *Proceedings of the 31st ACM International Conference on Multimedia*. 2795–2806.
- [53] Tian Ye, Sixiang Chen, Yun Liu, Yi Ye, Erkang Chen, and Yuche Li. 2022. Underwater light field retention: Neural rendering for underwater imaging. In *Proceedings of the IEEE/CVF Conference on Computer Vision and Pattern Recognition*. 488–497.
- [54] Xunpeng Yi, Han Xu, Hao Zhang, Linfeng Tang, and Jiayi Ma. 2023. Diff-Retinex: Rethinking Low-light Image Enhancement with A Generative Diffusion Model. *CoRR abs/2308.13164* (2023).
- [55] Syed Waqas Zamir, Aditya Arora, Salman Khan, Munawar Hayat, Fahad Shahbaz Khan, and Ming-Hsuan Yang. 2022. Restormer: Efficient transformer for high-resolution image restoration. In *Proceedings of the IEEE/CVF conference on computer vision and pattern recognition*. 5728–5739.
- [56] Richard Zhang, Phillip Isola, Alexei A. Efros, Eli Shechtman, and Oliver Wang. 2018. The Unreasonable Effectiveness of Deep Features as a Perceptual Metric. In *2018 IEEE Conference on Computer Vision and Pattern Recognition, CVPR 2018, Salt Lake City, UT, USA, June 18-22, 2018*. 586–595.
- [57] Chen Zhao, Weiling Cai, Chenyu Dong, and Chengwei Hu. 2024. Wavelet-based Fourier Information Interaction with Frequency Diffusion Adjustment for Underwater Image Restoration. In *Proceedings of the IEEE/CVF Conference on Computer Vision and Pattern Recognition (CVPR)*.
- [58] Chen Zhao, Weiling Cai, Chenyu Dong, and Ziqi Zeng. 2023. Toward Sufficient Spatial-Frequency Interaction for Gradient-aware Underwater Image Enhancement. *arXiv preprint arXiv:2309.04089* (2023).
- [59] Yu Zheng, Jiahui Zhan, Shengfeng He, Junyu Dong, and Yong Du. 2023. Circular contrastive regularization for physics-aware single image dehazing. In *Proceedings of the IEEE/CVF conference on computer vision and pattern recognition*. 5785–5794.
- [60] Dewei Zhou, You Li, Fan Ma, Zongxin Yang, and Yi Yang. 2024. MIGC: Multi-Instance Generation Controller for Text-to-Image Synthesis. *arXiv preprint arXiv:2402.05408* (2024).
- [61] Dewei Zhou, Zongxin Yang, and Yi Yang. 2023. Pyramid diffusion models for low-light image enhancement. *arXiv preprint arXiv:2305.10028* (2023).